

Magnetic properties and ^{155}Gd Mössbauer spectroscopy of the rare-earth Heusler compound Cu_2GdIn

Pu Wang and Zbigniew M Stadnik¹

Department of Physics, University of Ottawa, Ottawa, ON, K1N 6N5, Canada

E-mail: stadnik@uottawa.ca

Received 28 May 2007, in final form 10 July 2007

Published 31 July 2007

Online at stacks.iop.org/JPhysCM/19/346235

Abstract

The results of x-ray diffraction, magnetic susceptibility, and ^{155}Gd Mössbauer spectroscopy studies of the rare-earth Heusler compound Cu_2GdIn are reported. The studied compound has the $L2_1$ crystal structure with the lattice constant of 0.666 43(3) nm. Cu_2GdIn is an antiferromagnet with the Néel temperature $T_N = 9.6(1)$ K. The temperature dependence of the magnetic susceptibility above T_N follows the Curie–Weiss law with the effective magnetic moment of 7.98(4) μ_B per Gd atom and the paramagnetic Curie temperature of $-41.2(9)$ K. The Debye temperature of Cu_2GdIn is 229(5) K. The temperature dependence of the hyperfine magnetic field follows a $J = 7/2$ Brillouin function. It is shown that the total contribution to the hyperfine magnetic field at ^{155}Gd nuclei in Gd-containing Heusler compounds resulting from the conduction electron polarization is +9.8(2.5) T.

(Some figures in this article are in colour only in the electronic version)

1. Introduction

Heusler compounds are ternary intermetallic compounds having the general composition X_2YZ . In the traditional Heusler compounds, X and Y stand for d-electron transition metals and Z denotes an sp-electron element [1]. These compounds possess the characteristic $L2_1$ crystal structure (space group $Fm\bar{3}m$, No 225) with the unit cell consisting of four interpenetrating face-centred cubic sub-lattices. They have been extensively investigated for their magnetic properties [1]. The majority of these traditional Heusler compounds are ferromagnets and some of them order antiferromagnetically [1].

¹ Author to whom any correspondence should be addressed.

There is a small number of Heusler compounds in which Y is a rare earth element, R. These include the most intensively studied system Pd₂RSn (R = Tb–Lu) [2–18], Pd₂RIn (R = La, Gd, Ho, Yb, Lu) [19–23], Pd₂RPb (R = Gd–Lu) [24], Pd₂RSb (R = Gd–Er) [25, 26], Pd₂RBi (R = Dy–Er) [25, 26], Au₂RIn (R = La–Nd, Er–Yb) [27, 28], Ag₂RIn (R = La–Nd, Sm, Gd–Yb) [29–33], and Cu₂RIn (R = La–Nd, Sm, Gd–Er, Lu) [34–41]. In contrast to the traditional Heusler compounds, the majority of rare-earth Heusler compounds are antiferromagnets [3, 5, 7–9, 13, 15, 24, 25, 30–33, 35, 36, 38–41].

In this paper we report on an investigation of magnetism of the Heusler compound Cu₂GdIn through measurements of magnetic susceptibility and ¹⁵⁵Gd Mössbauer spectroscopy.

2. Experimental procedure

An ingot of nominal composition Cu₂GdIn was prepared by melting constituent elements in an induction furnace on a water-cooled Cu boat under an Ar atmosphere. Purities of the starting elements were 99.999%, 99.999%, and 99.998% for Cu, In, and Gd, respectively. The melting was repeated four times, in each case after turning the ingot over. The total weight loss after the melting was 1.1%.

X-ray diffraction measurement was performed at 298 K in Bragg–Brentano geometry on the PANanalytical X'Pert scanning diffractometer using Cu K α radiation. The K β line was eliminated by using a Kevex PSI2 Peltier-cooled solid-state Si detector. In order to avoid the deviation from intensity linearity of the solid-state Si detector, its parameters and the parameters of the diffractometer were chosen in such a way as to limit the count rate from the most intense Bragg peaks to less than 9000 counts s⁻¹ [42].

The magnetic susceptibility was measured with a Quantum Design superconducting quantum interference device magnetometer at various fields in the temperature range 4.5–295 K.

The ¹⁵⁵Gd MS measurements in the temperature range 1.5–20.0 K were conducted using a standard Mössbauer spectrometer operating in a sine mode and a source of ¹⁵⁵Eu(SmPd₃). The source was kept at the same temperature as that of the absorber. The spectrometer was calibrated with a Michelson interferometer [43], and the spectra were folded. The Mössbauer absorber was made of pulverized material pressed into a pellet which was then put into an Al disk container of thickness 0.008 mm to ensure a uniform temperature over the whole sample. The surface density of the Mössbauer absorber of the studied compound was 352 mg cm⁻². The 86.5 keV γ -rays were detected with a 2.5 cm NaI(Tl) scintillation detector covered with a 0.6 mm Pb plate to cut off the 105.3 keV γ -rays emitted from the source.

The Mössbauer spectra were analyzed by means of a least-squares fitting procedure which entailed calculations of the positions and relative intensities of the absorption lines by numerical diagonalization of the full hyperfine interaction Hamiltonian. The interference ξ factor for the E1 transition of 86.5 keV in ¹⁵⁵Gd was fixed to the value of 0.0520, which was derived from the fit of the ¹⁵⁵Gd Mössbauer spectrum of GdFe₂ at 4.2 K (data not shown here). The resonance line shape of the Mössbauer spectra was described by a transmission integral formula [44, 45]. In addition to the hyperfine parameters, only the absorber Debye–Waller factor f_a and the absorber linewidth Γ_a were fitted as independent parameters. The source linewidth $\Gamma_s = 0.334$ mm s⁻¹ and the background-corrected Debye–Waller factor of the source f_s^* [44, 45], which were derived from the fit of the ¹⁵¹Gd Mössbauer spectrum of GdFe₂ at 4.2 K, were used. The ¹⁵⁵Eu(SmPd₃) source at 1.5 K emits a broadened emission line; from the fit of the ¹⁵¹Gd Mössbauer spectrum of GdFe₂ at 1.5 K we found that $\Gamma_s = 0.708$ mm s⁻¹.

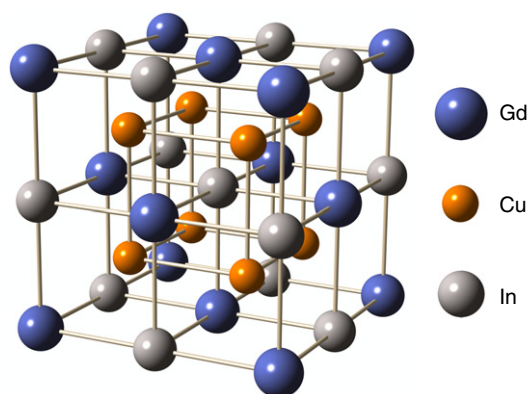


Figure 1. Heusler L_{21} crystal structure of Cu_2GdIn .

Table 1. Crystallographic data for Cu_2GdIn .

Atom	Site	Point symmetry	x	y	z	Occupancy
Gd	4a	$m\bar{3}m$	0	0	0	1.0
In	4b	$m\bar{3}m$	$\frac{1}{2}$	$\frac{1}{2}$	$\frac{1}{2}$	1.0
Cu	8c	$\bar{4}3m$	$\frac{1}{4}$	$\frac{1}{4}$	$\frac{1}{4}$	1.0

3. Results and discussion

3.1. Structural characterization

The compound Cu_2GdIn forms in the L_{21} crystal structure with the space group $Fm\bar{3}m$ (No 225). Figure 1 shows the crystal structure of Cu_2GdIn , and the crystallographic data for the Gd, In, and Cu sites are given in table 1.

The x-ray powder diffraction pattern of Cu_2GdIn is shown in figure 2. A Rietveld refinement of the x-ray powder diffraction data was performed, yielding the lattice constant $a = 0.66643(3)$ nm. The studied sample contains a trace of Cu_4GdIn second phase in the amount of 3.7(5) wt% as determined from the Rietveld refinement of the x-ray powder diffraction pattern (figure 2). The studied Heusler compound Cu_2GdIn could be thus slightly off stoichiometry.

3.2. Magnetic susceptibility

The temperature dependence of the magnetic susceptibility χ of Cu_2GdIn measured in an applied magnetic field of 0.5 T between 4.5 and 295 K is shown in figure 3(a). The $\chi(T)$ curve exhibits a sharp peak at 9.6(1) K (inset in figure 3(a)). This indicates that Cu_2GdIn is an antiferromagnet with the Néel temperature $T_N = 9.6(1)$ K.

The $\chi(T)$ data above 100 K could be fitted to a modified Curie–Weiss law

$$\chi = \chi_0 + \frac{C}{T - \theta_p}, \quad (1)$$

where χ_0 is the temperature independent magnetic susceptibility, C is the Curie constant, and θ_p is the paramagnetic Curie temperature. The Curie constant can be expressed as $C = \frac{N\mu_{\text{eff}}^2}{3k}$, where N is the concentration of magnetic atoms per unit mass and μ_{eff} is the effective magnetic moment. Figure 3(b) shows the inverse magnetic susceptibility corrected for the contribution

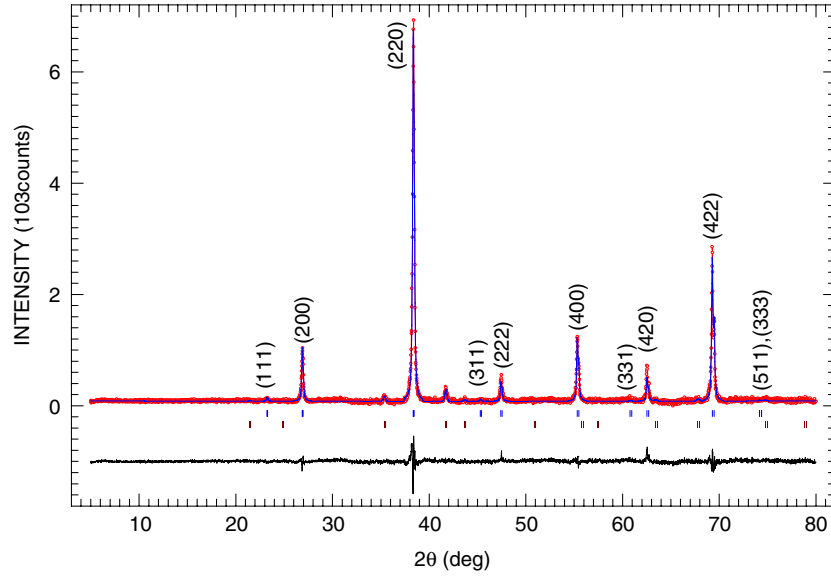


Figure 2. The x-ray powder diffraction spectrum of Cu_2GdIn at 298 K. The experimental data are denoted by open circles, while the line through the data represents the results of the Rietveld refinement. The upper set of vertical bars represents the Bragg peak positions corresponding to the principal Cu_2GdIn phase, while the lower set refers to the positions of the minor impurity Cu_4GdIn phase. The lower curve is the difference curve between the experimental data and the calculated curve.

χ_0 , $(\chi - \chi_0)^{-1}$ versus temperature; the validity of the Curie–Weiss law is evident. The values of χ_0 , C , and θ_p obtained from the fit are, respectively, $5.50(17) \times 10^{-6} \text{ emu g}^{-1}$, $19.94(20) \times 10^{-3} \text{ emu K g}^{-1}$, and $-41.2(9) \text{ K}$. This value of C corresponds to μ_{eff} of $7.98(4) \mu_B$ per Gd atom.

For a free Gd^{3+} ion (electronic ground state $^8S_{7/2}$), the theoretical value of $\mu_{\text{eff}}^{\text{th}} = g\mu_B\sqrt{J(J+1)}$ is $7.94 \mu_B$ [46]. The fact that the experimental value $\mu_{\text{eff}} = 7.98(4) \mu_B$ is very close to the theoretical value of $7.94 \mu_B$ confirms that the magnetic moment is localized on the Gd^{3+} ions and that, as expected, Cu and In atoms carry no magnetic moment. The negative value of θ_p indicates the predominantly antiferromagnetic interaction between the Gd^{3+} spins.

3.3. Mössbauer spectroscopy

Figure 4 displays ^{151}Gd Mössbauer spectra of Cu_2GdIn measured at temperatures above the Néel temperature. The Gd^{3+} ions are located in the Heusler structure at the site with the point symmetry $m\bar{3}m$ (table 1). This ensures a zero electric field gradient at the Gd^{3+} site and hence zero electric quadrupole splitting. The spectra in figure 4 exhibit thus no electric quadrupole interaction and are fitted with a single line. The parameters derived from the fits are given in table 2.

The values of the isomer shift (relative to the $^{155}\text{Eu}(\text{SmPd}_3)$ source) δ of $\sim 0.42 \text{ mm s}^{-1}$ are characteristic for Gd atoms being in a trivalent state [47]. In terms of the Debye approximation of the lattice vibrations, the absorber Debye–Waller factor f_a is expressed [48, 49] by the Debye temperature, Θ_D , as

$$f_a(T) = \exp \left\{ -\frac{3}{4} \frac{E_\gamma^2}{Mc^2k\Theta_D} \left[1 + \left(\frac{T}{\Theta_D} \right)^2 \int_0^{\Theta_D/T} \frac{x dx}{e^x - 1} \right] \right\}, \quad (2)$$

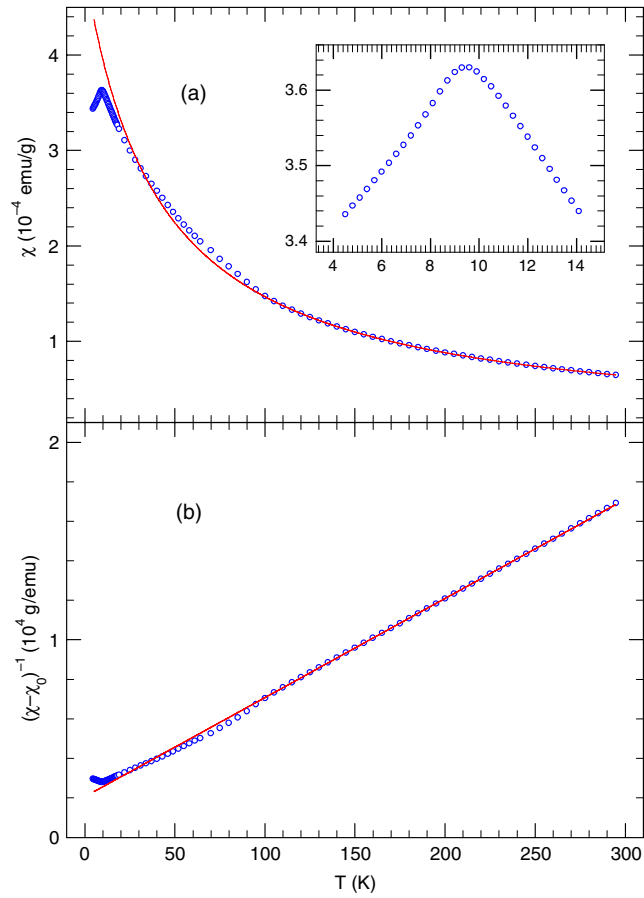


Figure 3. (a) The temperature dependence of the magnetic susceptibility of Cu_2GdIn , measured in an external magnetic field of 0.5 T. The solid line is the fit to equation (1) in the temperature range 100–295 K. The temperature dependence of the magnetic susceptibility in the low-temperature range is presented in the inset. (b) The inverse magnetic susceptibility corrected for the contribution χ_0 , $(\chi - \chi_0)^{-1}$ versus temperature T of Cu_2GdIn . The solid line is the fit to equation (1) in the temperature range 100–295 K.

Table 2. Hyperfine interaction parameters derived from the fits to the ^{151}Gd Mössbauer spectra of Cu_2GdIn at various temperatures.

T (K)	δ (mm s $^{-1}$)	Γ_a (mm s $^{-1}$)	H_{hf} (T)	f_a (%)	χ^2
20.0	0.405(3)	0.408(10)		12.6(3)	1.00
12.6	0.415(4)	0.425(12)		13.3(3)	1.01
10.2	0.422(4)	0.460(13)		13.7(4)	1.13
9.1	0.406(3)	0.460(12)	6.62(32)	13.7(3)	0.91
8.1	0.421(4)	0.461(11)	12.51(22)	13.8(3)	1.01
7.0	0.405(4)	0.461(10)	16.37(20)	12.8(4)	1.03
5.9	0.414(3)	0.461(12)	18.51(15)	13.8(3)	1.15
4.9	0.407(4)	0.460(13)	20.56(16)	13.8(4)	1.20
1.5	0.414(5)	0.462(14)	22.72(27)	13.9(4)	1.17

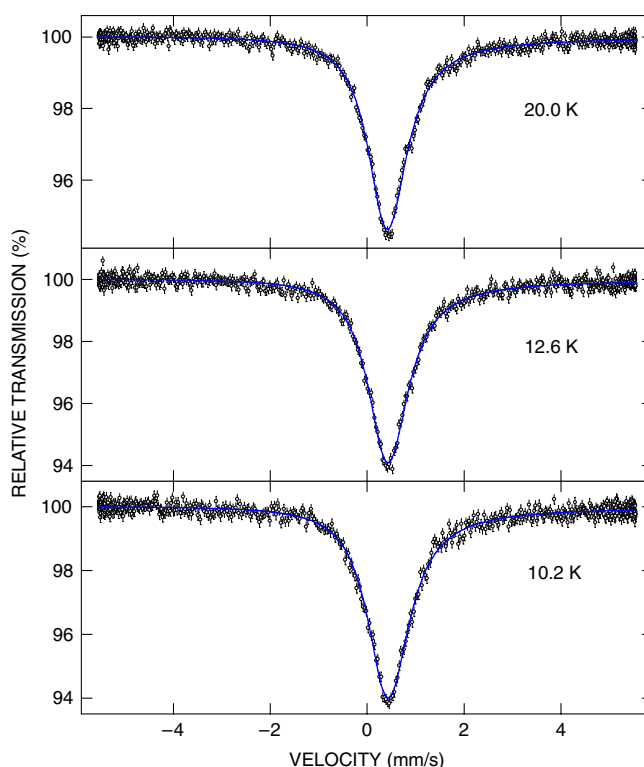


Figure 4. ^{155}Gd Mössbauer spectra of Cu_2GdIn at various temperatures above the Néel temperature. Solid lines are fits, as described in the text. The zero-velocity scale is relative to the source.

where E_γ is the energy of the Mössbauer transition, M is the mass of the Mössbauer nucleus, c is the speed of light, and k is the Boltzmann constant. The analysis of the values of f_a given in table 2 via equation (2) yields $\Theta_D = 229(5)$ K. This value compares well with $\Theta_D = 183$ K for an isostructural Heusler compound Cu_2LaIn [50].

^{151}Gd Mössbauer spectra of Cu_2GdIn measured at temperatures below the Néel temperature are shown in figure 5. They exhibit the presence of a magnetic dipole hyperfine interaction. It is not visually obvious that the ^{151}Gd Mössbauer spectrum at 9.1 K results from a non-zero magnetic dipole hyperfine interaction, i.e., that the non-zero hyperfine magnetic field, H_{hf} , sets in. The 9.1 K spectrum looks like a single-line spectrum, similar to those shown in figure 4. The fit of this spectrum with a single line yields $\Gamma_a = 0.539(9)$ mm s^{-1} and $\chi^2 = 0.99$. A substantial increase of Γ_a from 0.460(13) mm s^{-1} for the 8.0 K spectrum (table 2) to 0.539(9) mm s^{-1} for the 9.1 K spectrum proves that indeed the observed broadening results from the non-zero H_{hf} being established in the 9.1 K spectrum. In addition, the value of $\chi^2 = 0.91$ obtained for the fit of the 9.1 K spectrum with a Zeeman pattern (table 2) is smaller than the value of 0.99 obtained for a single-line fit. The parameters derived from the fits of the spectra in figure 5 with a non-zero magnetic dipole hyperfine interaction are given in table 2.

Figure 6 shows the temperature dependence of the hyperfine magnetic field determined from the fits of the spectra in figure 5. The hyperfine magnetic field is generally proportional to the magnetic moment of Gd atoms. Its temperature dependence will reflect the latter and follows a Brillouin function [46]. The temperature dependence of $H_{\text{hf}}(T)$ can thus be

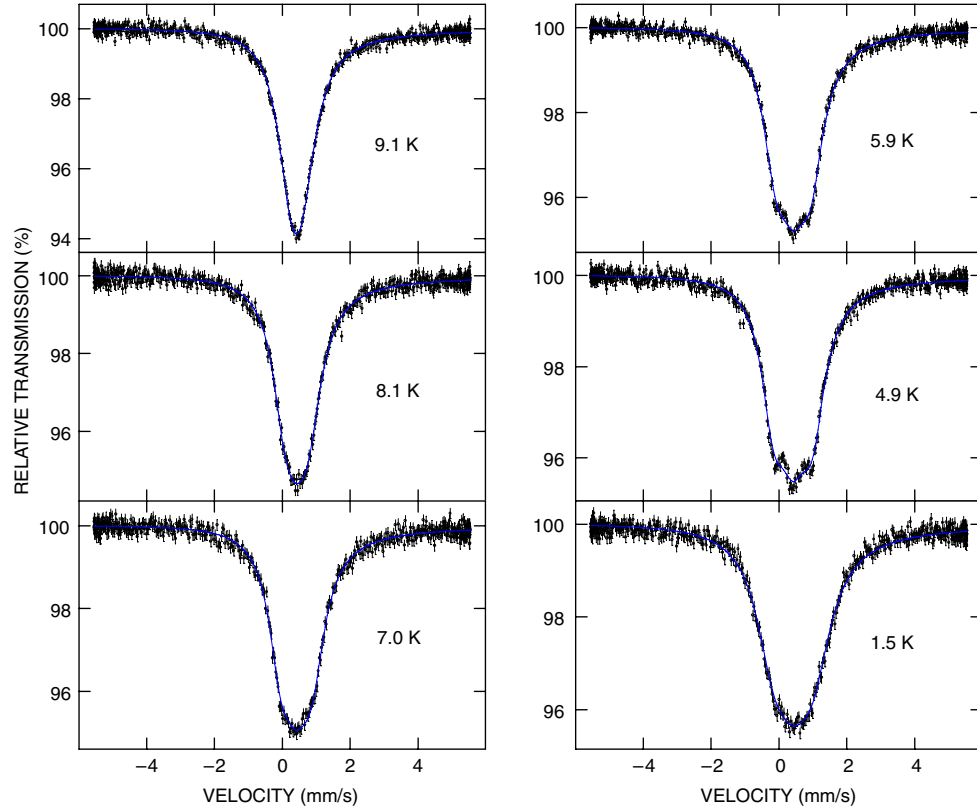


Figure 5. ^{155}Gd Mössbauer spectra of Cu_2GdIn at various temperatures below the Néel temperature. Solid lines are fits, as described in the text. The zero-velocity scale is relative to the source.

expressed as

$$H_{\text{hf}}(T) = H_{\text{hf}}(0)B_J(x), \quad (3)$$

where $H_{\text{hf}}(0)$ is the saturation hyperfine magnetic field, $B_J(x)$ is the Brillouin function defined as

$$B_J(x) = \frac{2J+1}{2J} \coth\left(\frac{2J+1}{2J}x\right) - \frac{1}{2J} \coth\left(\frac{x}{2J}\right) \quad (4)$$

and

$$x = \frac{3J}{J+1} \frac{H_{\text{hf}}(T) T_{\text{N}}}{H_{\text{hf}}(0) T}. \quad (5)$$

A least-squares fit of the $H_{\text{hf}}(T)$ data to equation (3) with $J = 7/2$ yields $H_{\text{hf}}(0) = 23.68(25)$ T and $T_{\text{N}} = 9.5(1)$ K. The value of T_{N} determined from the fit is in excellent agreement with the value determined from the susceptibility measurement.

The hyperfine magnetic field at the ^{155}Gd nuclei in Cu_2GdIn can be expressed as the sum of three terms

$$H_{\text{hf}} = H_{\text{cp}} + H_{\text{s}} + H_{\text{tr}}. \quad (6)$$

The core polarization field, H_{cp} , is due to the exchange interaction between the local Gd 4f electrons and the core electrons. Its value, $-34.0(2.0)$ T [51–53], is assumed to be independent

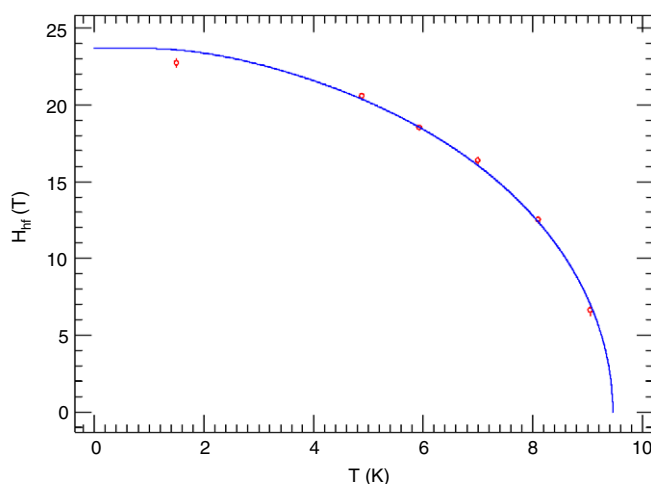


Figure 6. The temperature dependence of the hyperfine magnetic field of Cu_2GdIn . The solid line is the fit to a $J = 7/2$ Brillouin function (equation (3)), as explained in the text.

of the Gd environment in solids. The negative sign arises from the fact that H_{cp} is antiparallel to the parent Gd 4f magnetic moment. The self-polarization term, H_s , results from the conduction electron polarization by the spin of the parent Gd atom and is usually parallel to the Gd magnetic moment. The transferred field, H_{tr} , is due to the conduction electron polarization by the surrounding Gd spins. For collinear magnetic structure, it is parallel to the Gd magnetic moment. In the absence of an externally applied magnetic field, one cannot determine the sign of the measured H_{hf} . However, in many Gd compounds the sign of H_{hf} was demonstrated to be negative [54–57]. Assuming thus that $H_{\text{hf}}(0) = -23.68(25)$ T allows one by using equation (6) to determine the total contribution from the conduction electron polarization $H_s + H_{\text{tr}}$ to be $+10.32(2.25)$ T.

The magnitude of the hyperfine magnetic field at the ^{155}Gd nuclei in an isostructural Heusler compound Ag_2GdIn at 4.2 K is $24.8(8)$ T [58]. By using the same analysis as above, one finds that in Ag_2GdIn the total contribution from the conduction electron polarization is $+9.2(2.8)$ T. One can thus conclude that the total contribution to the hyperfine magnetic field at the ^{155}Gd nuclei from the conduction electron polarization in Gd-containing Heusler compounds is $+9.8(2.5)$ T.

4. Conclusions

A rare-earth Heusler compound Cu_2GdIn has been studied with x-ray diffraction, magnetic susceptibility, and ^{155}Gd Mössbauer spectroscopy. This compound has the $L2_1$ crystal structure with the lattice constant of $6.6643(3)$ Å. Gd magnetic moments order antiferromagnetically with the Néel temperature $T_N = 9.6(1)$ K. The temperature dependence of the magnetic susceptibility above T_N follows the Curie–Weiss law with the effective magnetic moment of $7.98(4)$ μ_B per Gd atom and the paramagnetic Curie temperature of $-41.2(9)$ K. The Debye temperature of Cu_2GdIn is $229(5)$ K. The temperature dependence of the hyperfine magnetic field at the ^{155}Gd nuclei follows a $J = 7/2$ Brillouin function and the saturation hyperfine magnetic field is $-23.68(25)$ T. It is shown that total contribution to the hyperfine magnetic field at ^{155}Gd nuclei in Gd-containing Heusler compounds resulting from the conduction electron polarization is $+9.8(2.5)$ T.

Acknowledgment

This work was supported by the Natural Sciences and Engineering Research Council of Canada.

References

- [1] Webster P J and Ziebeck K R A 1988 *Magnetic Alloy and Compounds of d-Elements with Main Group Elements (Landolt-Börnstein New Series Group III, vol 19c)* ed H P J Wijn (Berlin: Springer) p 75
Ziebeck K R A and Neuman K-U 2001 *Magnetic Properties of Metals (Landolt-Börnstein New Series Group III, vol 32)* ed H P J Wijn (Berlin: Springer) p 64
- [2] Johnson M J and Shelton R N 1984 *Solid State Commun.* **52** 839
- [3] Malik S K, Umarji A M and Shenoy G K 1985 *Phys. Rev. B* **31** 6971
- [4] Kierstead H A, Dunlap B D, Malik S K, Umarji A M and Shenoy G K 1985 *Phys. Rev. B* **32** 135
- [5] Umarji A M, Malik S K and Shenoy G K 1985 *Solid State Commun.* **53** 1029
- [6] Shelton R N, Hausermann-Berg L S, Johnson M J, Klavins P and Yang H D 1986 *Phys. Rev. B* **34** 199
- [7] Malik S K, Umarji A M and Shenoy G K 1986 *Phys. Rev. B* **34** 3144
- [8] Stanley H B, Lynn J W, Shelton R N and Klavins P 1987 *J. Appl. Phys.* **61** 3371
- [9] Donaberger R L and Stager C V 1987 *J. Less-Common Met.* **127** 93
- [10] Li W-H, Lynn J W, Stanley H B, Udovic T J, Shelton R N and Klavins P 1989 *Phys. Rev. B* **39** 4199
- [11] Crangle J, Neumann K-U, Smith J G and Ziebeck K R A 1995 *J. Magn. Magn. Mater.* **140-144** 919
- [12] Babateen M, Neumann K-U and Ziebeck K R A 1995 *J. Magn. Magn. Mater.* **140-144** 921
- [13] Parsons M J, Crangle J, Dennis B, Neumann K-U and Ziebeck K R A 1996 *Czech. J. Phys.* **46** (Suppl. S4) 2059
- [14] Aoki Y, Sato H R, Matsuda T D, Sugawara H and Sato H 1998 *J. Magn. Magn. Mater.* **177-181** 559
- [15] Dönni A, Fischer P, Fauth F, Convert P, Aoki Y, Sugawara H and Sato H 1999 *Physica B* **259-261** 705
- [16] Aoki Y, Sato H R, Sugawara H and Sato H 2000 *Physica C* **333** 187
- [17] Amato A, Roessli B, Fischer P, Bernhoeft N, Stunault A, Baines C, Dönni A and Sugawara H 2003 *Physica B* **326** 369
- [18] Giudicelli P, Roessli B, Stunault A, Ollivier J, Amato A, Sugawara H and Bernhoeft N 2004 *J. Magn. Magn. Mater.* **272-276** e141
- [19] Neumann K-U, Crangle J, Giles R T, Visser D, Zayer N K and Ziebeck K R A 1992 *Solid State Commun.* **84** 577
- [20] Babateen M, Crangle J, Fauth F, Furrer A, Neumann K-U and Ziebeck K R A 1995 *Physica B* **213/214** 300
- [21] Parsons M J, Crangle J, Dennis B, Neumann K-U and Ziebeck K R A 1996 *Czech. J. Phys.* **46** (Suppl. S4) 2057
- [22] Parsons M J, Crangle J, Neumann K-U and Ziebeck K R A 1998 *J. Magn. Magn. Mater.* **184** 184
- [23] Taylor J W, Capellmann H, Neumann K-U and Ziebeck K R A 2000 *Eur. Phys. J. B* **16** 233
- [24] Seaman C L, Dilley N R, de Andrade M C, Herrmann J, Maple M B and Fisk Z 1996 *Phys. Rev. B* **53** 2651
- [25] Gofryk K, Kaczorowski D, Plackowski T, Leithe-Jasper A and Grin Yu 2005 *Phys. Rev. B* **72** 094409
- [26] Kaczorowski D, Gofryk K, Plackowski T, Leithe-Jasper A and Grin Yu 2005 *J. Magn. Magn. Mater.* **290/291** 573
- [27] Wernick J H, Hull G W, Geballe T H, Bernardini J E and Waszczak J V 1983 *Mater. Lett.* **2** 90
- [28] Kurisu M, Fuse A, Nobata T and Nakamoto G 2000 *Physica B* **281/282** 147
- [29] Lal H B and Methfessel S 1981 *J. Magn. Magn. Mater.* **23** 283
- [30] Galera R M, Pierre J and Pannetier J 1982 *J. Phys. F: Met. Phys.* **12** 993
- [31] Galera R M, Pierre J, Siaud E and Murani A P 1984 *J. Less-Common Met.* **97** 151
- [32] Lahiouel R, Pierre J, Siaud E and Murani A P 1987 *J. Magn. Magn. Mater.* **63/64** 104
- [33] Lahiouel R, Pierre J, Siaud E, Galera R M, Besnus M J, Kappler J P and Murani A P 1987 *Z. Phys.* **67** 185
- [34] Ōnuki Y, Yamazaki T, Kobori A, Omi T, Komatsubara T, Takayanagi S, Kato H and Wada N 1987 *J. Phys. Soc. Japan* **56** 4251
- [35] Takagi S, Kimura T, Sato N, Satoh T and Kasuya T 1988 *J. Phys. Soc. Japan* **57** 1562
- [36] Nakamura N, Kitaoka Y, Asayama K, Ōnuki Y and Komatsubara T 1988 *J. Phys. Soc. Japan* **57** 2276
- [37] Sato K, Mizushima T, Kondo K, Ishikawa Y, Mori K and Umehara I 1991 *J. Appl. Phys.* **69** 4645
- [38] Felner I 1985 *Solid State Commun.* **56** 315
- [39] Neumann K-U, Crangle J, Visser D, Zayer N K and Ziebeck K R A 1993 *Phys. Lett. A* **177** 99
- [40] Rotter M, Loewenhaupt M, Doerr M, Lindbaum A, Sassik H, Ziebeck K and Beuneu B 2003 *Phys. Rev. B* **68** 144418
- [41] Rotter M, Doerr M, Loewenhaupt M, Lindbaum A, Ziebeck K and Beuneu B 2004 *Physica B* **350** e63
- [42] Bish D L and Chipera S J 1989 *Powder Diffr.* **4** 137
- [43] Otterloo B F, Stadnik Z M and Swolfs A E M 1983 *Rev. Sci. Instrum.* **54** 1575
- [44] Margulies S and Ehrman J R 1961 *Nucl. Instrum. Methods* **12** 131

- [45] Shenoy G K, Friedt J M, Maletta H and Ruby S L 1974 *Mössbauer Effect Methodology* vol 10 , ed I J Gruverman, C W Seidel and D K Dieterly (New York: Plenum) p 277
- [46] Blundell S 2001 *Magnetism in Condensed Matter* (Oxford: Oxford University Press)
- [47] Bauminger E R, Kalvius G M and Nowik I 1978 *Mössbauer Isomer Shifts* ed G K Shenoy and F E Wagner (Amsterdam: North-Holland) p 661
- [48] Greenwood N N and Gibb T C 1971 *Mössbauer Spectroscopy* (London: Chapman and Hall)
- [49] Gütlich P, Link R and Trautwein A 1978 *Mössbauer Spectroscopy and Transition Metal Chemistry* (Berlin: Springer)
- [50] Sato K, Ishikawa Y and Mori K 1992 *J. Magn. Magn. Mater.* **104–107** 1435
- [51] Gegenwarth R E, Budnick J I, Skalski S and Wernick J H 1967 *Phys. Rev. Lett.* **18** 9
- [52] Hüfner S and Wernick J H 1968 *Phys. Rev.* **173** 448
- [53] Khoi L D 1969 *Phys. Lett. A* **28** 671
- [54] Jeandey C, Oddou J L, Boucher B, Tourbot R and Czjzek G 1967 *J. Magn. Magn. Mater.* **89** 335
- [55] Ruebenbauer K, Fink J, Schmidt H, Czjzek G and Tomala K 1977 *Phys. Status Solidi b* **84** 611
- [56] Sanchez J P, Tomala K and Szytula A 1991 *Solid State Commun.* **78** 419
- [57] Malaman B, Venturini G, Welter R, Sanchez J P, Vulliet P and Ressouche E 1999 *J. Magn. Magn. Mater.* **202** 519
- [58] De Vries J W C, Thiel R C and Buschow K H J 1985 *J. Less-Common Met.* **111** 313